

# Within-plant isoprene oxidation confirmed by direct emissions of oxidation products methyl vinyl ketone and methacrolein

KOLBY J. JARDINE\*, RUSSELL K. MONSON†, LEIF ABRELL‡§, SCOTT R. SALESKA¶, ALMUT ARNETH\*\*††, ANGELA JARDINE\*, FRANÇOISE YOKO ISHIDA‡‡, ANA MARIA YANEZ SERRANO‡‡, PAULO ARTAXO§§, THOMAS KARL¶¶, SILVANO FARES\*\*\*, ALLEN GOLDSTEIN†††, FRANCESCO LORETO‡‡‡ and TRAVIS HUXMAN\*¶

\*The University of Arizona-Biosphere 2, PO Box 8746, Tucson, AZ 85738, USA, †School of Natural Resources and the Environment, University of Arizona, Biological Sciences East, Tucson, AZ 85721, USA, ‡Department of Chemistry & Biochemistry, University of Arizona, P.O. Box 210041, 1306 East University Blvd., Tucson, AZ 85721-0041, USA, §Department of Soil, Water & Environmental Science, University of Arizona, P.O. Box 210038, Tucson, AZ 85721-0038, USA, ¶Department of Ecology and Evolutionary Biology, University of Arizona, P.O. Box 210088, BioSciences West 310, Tucson, AZ 85721, USA, \*\*Department of Physical Geography and Ecosystems Analysis, Lund University, Sölvegatan 12, S-223 62, Lund, Sweden, ††Research Centre Karlsruhe, Institute for Meteorology and Climate Research (IMK-IFU), 82467, Garmisch-Partenkirchen, Germany, ‡‡Large Biosphere-Atmosphere Experiment (LBA), Instituto Nacional de Pesquisas da Amazônia, Av. André Araújo, 2936, Aleixo, CEP 69060-001, Manaus, Brazil, §§Instituto de Física Rua do Matao, Universidade de São Paulo, Travessa R Nr. 187, CEP 05508-090, Cidade Universitária, São Paulo, Brazil, ¶¶Atmospheric Chemistry Division, National Center for Atmospheric Research, P.O. Box 3000, Boulder, CO 80307-3000, USA, \*\*\*Agricultural Research Council (CRA), Research Center for the Soil Plant System, Via della Navicella 2-4, 00184, Rome, Italy, †††Department of Environmental Science, Policy, and Management, University of California, 130 Mulford Hall #3114, Berkeley, CA 94720, USA, ‡‡‡National Research Council, Institute for Plant Protection, Via Madonna del Piano 10, 50132, Sesto Fiorentino (Firenze), Italy

## Abstract

Isoprene is emitted from many terrestrial plants at high rates, accounting for an estimated 1/3 of annual global volatile organic compound emissions from all anthropogenic and biogenic sources combined. Through rapid photooxidation reactions in the atmosphere, isoprene is converted to a variety of oxidized hydrocarbons, providing higher order reactants for the production of organic nitrates and tropospheric ozone, reducing the availability of oxidants for the breakdown of radiatively active trace gases such as methane, and potentially producing hygroscopic particles that act as effective cloud condensation nuclei. However, the functional basis for plant production of isoprene remains elusive. It has been hypothesized that in the cell isoprene mitigates oxidative damage during the stress-induced accumulation of reactive oxygen species (ROS), but the products of isoprene-ROS reactions in plants have not been detected. Using pyruvate-<sup>2-13</sup>C leaf and branch feeding and individual branch and whole mesocosm flux studies, we present evidence that isoprene (*i*) is oxidized to methyl vinyl ketone and methacrolein (*i<sub>ox</sub>*) in leaves and that *i<sub>ox</sub>*/*i* emission ratios increase with temperature, possibly due to an increase in ROS production under high temperature and light stress. In a primary rainforest in Amazonia, we inferred significant in plant isoprene oxidation (despite the strong masking effect of simultaneous atmospheric oxidation), from its influence on the vertical distribution of *i<sub>ox</sub>* uptake fluxes, which were shifted to low isoprene emitting regions of the canopy. These observations suggest that carbon investment in isoprene production is larger than that inferred from emissions alone and that models of tropospheric chemistry and biota–chemistry–climate interactions should incorporate isoprene oxidation within both the biosphere and the atmosphere with potential implications for better understanding both the oxidizing power of the troposphere and forest response to climate change.

**Keywords:** Amazon, biosphere–atmosphere interactions, isoprene oxidation, methacrolein, methyl vinyl ketone, reactive oxygen species, temperature stress, thermotolerance

Received 18 October 2011; revised version received 18 October 2011 and accepted 3 November 2011

Correspondence: Kolby J. Jardine, tel. + 520 603 6096, fax + 520 838 6162, e-mail: jardine@email.arizona.edu

## Introduction

The oxidative power of the lower atmosphere is controlled to a large extent by the emission of biogenic hydrocarbons, especially those that contain carbon–carbon double bonds, and is thus available for oxidation through reaction with hydroxyl radicals, ozone, and nitrate radicals (Monson, 2002). The first-generation products formed from the oxidation of isoprene, the most abundantly emitted plant hydrocarbon, are dominated by methyl vinyl ketone and methacrolein, collectively referred to here as  $i_{ox}$  (Pierotti *et al.*, 1990). To date, it has been assumed that most of the  $i_{ox}$  in the atmosphere is produced by atmospheric oxidation of isoprene, at the expense of atmospheric oxidants (Pierotti *et al.*, 1990; Montzka *et al.*, 1993; Warneke *et al.*, 2001; Tani *et al.*, 2010). This assumption has influenced the form of the current generation of atmospheric chemistry models that are used to study issues ranging from the oxidizing capacity of the atmosphere (Stavrakou *et al.*, 2010), the production of tropospheric ozone (Dreyfus *et al.*, 2002), and the tropospheric lifetime of methane (Young *et al.*, 2009).

A wide variety of biotic (e.g. microbes, insects) and abiotic (e.g. thermal, radiative, drought) stressors cause accumulation of reactive oxygen species (ROS), including hydrogen peroxide, singlet oxygen, superoxide anion, and the hydroxyl radical, in plant tissues. Excessive ROS accumulation can overwhelm cellular antioxidant defenses, including enzyme-mediated ROS quenching reactions, antioxidant systems for ROS scavenging, and defense gene activation (Moller, 2001). Following ROS accumulation, extensive oxidation of important components such as nucleic acids, proteins, and lipids can further exacerbate ROS accumulation leading to programmed cell death (Apel & Hirt, 2004). Thus, plants with a diverse suite of antioxidant defenses are expected to better tolerate stressful environmental conditions such as those caused by high temperatures, an important environmental variable central to global climate change.

As recently reviewed (Vickers *et al.*, 2009), a variety of studies support the view that isoprene can protect plants from stress through an antioxidant effect. For example, it has been shown that ozone (Loreto *et al.*, 2001), hydrogen peroxide (Loreto & Velikova, 2001), singlet oxygen (Velikova *et al.*, 2004), and nitric oxide (Velikova *et al.*, 2005) are all quenched in the presence of isoprene. However, several different processes have been hypothesized to account for these observations, and evidence for a direct role of isoprene in reacting with reactive oxygen and nitrogen species within plants has not been obtained. In the case of isoprene, if liquid-phase and/or lipid-phase chemistry inside leaves

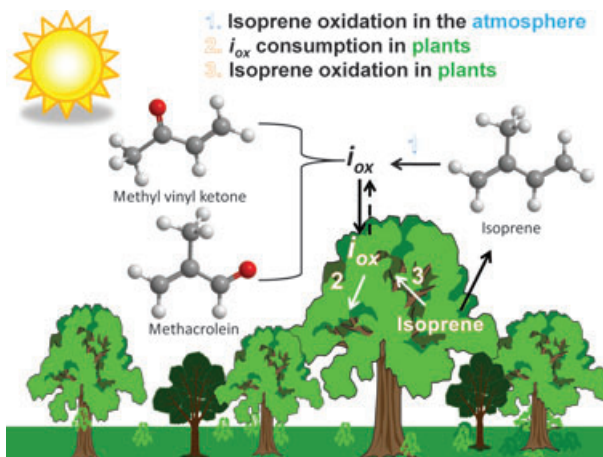


**Fig. 1** Simplified schematic of the biosphere–atmosphere exchange of isoprene and its oxidation products methyl vinyl ketone and methacrolein ( $i_{ox}$ ). Traditionally, isoprene emitted by plants is oxidized to  $i_{ox}$  in the troposphere (1). More recently, studies have also found an uptake of tropospheric  $i_{ox}$  by vegetation (2). Here, we argue for a third central process, namely the oxidation of isoprene to  $i_{ox}$  within the plant cell (3). Therefore, interpretation of  $i_{ox}$  concentrations in the atmosphere needs to consider all three processes.

results in the production of similar oxidation products as gas-phase chemistry in the atmosphere, the main oxidation products should be  $i_{ox}$  (Loreto & Schnitzler, 2010), which should carry carbon atoms derived from isoprene (Fig. 1). In this study, we show that primary emissions of  $i_{ox}$  occurs from a variety of isoprene emitting tropical plants and suggest that  $i_{ox}$  emissions are a result of isoprene oxidation by ROS within plants. Using pyruvate-2-<sup>13</sup>C leaf and branch feeding experiments, we tracked the <sup>13</sup>C-label into isoprene and  $i_{ox}$  during de-novo biosynthesis and oxidation reactions. Individual branches and ambient air from a tropical rainforest mesocosm were used to investigate the temperature sensitivity of isoprene oxidation in plants. We extend this analysis to a natural primary rainforest in the central Amazon where we investigate the relative importance of isoprene oxidation within plants and the atmosphere in contributing to biosphere–atmosphere exchange of  $i_{ox}$ . Our findings call into question the assumption that isoprene production rates in plants are equal to emission rates and that the isoprene produced is exclusively oxidized in the atmosphere.

## Materials and methods

### Proton transfer reaction-mass spectrometry (PTR-MS)

Leaf, branch, and ambient concentrations of isoprene and methyl vinyl ketone and methacrolein ( $i_{ox}$ ) were quantified

using a commercial high sensitivity PTR-MS (IONICON, Austria). The PTR-MS was operated in standard conditions with a drift tube voltage of 600 V and drift tube pressure of 2.0 mb. Optimization of PTR-MS conditions resulted in high sustained primary ion ( $\text{H}_3\text{O}^+$ ) intensity ( $2\text{--}4 \times 10^7$  counts per second) with low water cluster and  $\text{O}_2^+$  formation ( $<4\%$   $\text{H}_3\text{O}^+$ ). The following mass to charge ratios ( $m/z$ ) was sequentially monitored during each PTR-MS measurement cycle; 21 ( $\text{H}_3^{18}\text{O}^+$ ), 32 ( $\text{O}_2^+$ ), 37 ( $\text{H}_2\text{O-H}_3\text{O}^+$ ) with a dwell time of 20 ms each, and 69 (isoprene- $\text{H}^+$ ) and 71 ( $i_{\text{ox}}$ : methyl vinyl ketone- $\text{H}^+$ , methacrolein- $\text{H}^+$ ) with a dwell time of 5 s each. During pyruvate-2- $^{13}\text{C}$  leaf feeding studies, the ions corresponding to isotopologues with a single  $^{13}\text{C}$  atom were also monitored with a 5 s dwell time. These were detected at  $m/z$  70 ( $^{13}\text{C}$ -isoprene) and  $m/z$  72 ( $^{13}\text{C}$ - $i_{\text{ox}}$ ). Raw signals (counts per second, cps) were normalized by the adjusted primary ion signal (cps<sub>21</sub>) and background subtracted from measurements of ultra high purity nitrogen (Brazil) or zero air (Biosphere 2 and California) to obtain normalized counts per second [ncps, Eqn (1)]. The adjusted primary ion signal (cps<sub>21</sub>) was obtained by measuring the signal at  $m/z$  21 ( $\text{H}_3^{18}\text{O}^+$ ) and multiplying it by the oxygen isotopic ratio of a representative natural abundance water sample ( $^{16}\text{O}/^{18}\text{O} = 500$ ).

$$\text{ncps} = (\text{cps}/\text{cps}_{21})_{\text{sample}} - (\text{cps}/\text{cps}_{21})_{\text{background}} \quad (1)$$

Calibration slopes (ppbv/ncps) for isoprene were obtained at Biosphere 2 and in the field (Brazil) using the dynamic solution injection technique (Jardine *et al.*, 2010b). Solutions were prepared by diluting 5  $\mu\text{L}$  of an authentic standard in 100 mL of cyclohexane. The solution was injected into the mixing vial at 0.5, 1.0, 2.0, and 3.0  $\mu\text{L min}^{-1}$  (30 min each flow rate) with a constant dilution flow of 1.0 slpm ultra high purity nitrogen passing through. The calibration slope of methyl vinyl ketone was obtained at Biosphere 2, which was assumed to be identical to that of methacrolein. Concentrations were calculated by multiplying the calibration slope by ncps.

#### *Methyl vinyl ketone and methacrolein identification by thermal desorption GC-PTR-MS*

The GC-PTR-MS was used to qualitatively determine if the PTR-MS signal at  $m/z$  71 measured during the laboratory experiments in the Biosphere 2 rainforest mesocosm were due to methyl vinyl ketone and methacrolein ( $i_{\text{ox}}$ ). The technical details of GC-PTR-MS have been described in detail elsewhere (Warneke *et al.*, 2003). A Varian CP-3800 GC with sample pre-concentration trap (Agilent Technologies, Santa Clara, CA, USA) was used for this study. Ambient air samples from the tropical rainforest mesocosm were drawn into a hydrocarbon trap (carbopack C, carbopack B, carboxen 1000, carboxen 1001) held at 30 °C to avoid excessive water collection. Air samples were drawn into the trap at 40 sccm for 5 min using a mass flow controller and a pump downstream of the trap. The collected sample was then injected directly onto the analytical column (Rtx-Volatiles, 30 m, 0.25 mm ID, 1 micron film thickness, Restek Inc., Bellefonte, PA, USA) by rapidly heating the trap to 200 °C for 5 min with 1.5 sccm of UHP helium carrier gas.

After sample injection, the GC oven was held at 40 °C for 5 min and then heated 10 °C  $\text{min}^{-1}$  to 200 °C. The end of the column was connected to a 1/16 in O.D. Silcosteel<sup>®</sup> tube that extended out of the GC oven. Gas exiting the tubing was mixed with UHP nitrogen through a tee that was connected to the PTR-MS inlet. Upstream of this tee was a second tee that was overblown by 100 sccm UHP nitrogen. This allowed all of the compounds eluting from the column to be swept into the nitrogen air stream and carried into the PTR-MS which requires ~50 sccm. The ion set ( $m/z$  69, 71) was scanned by the quadrupole mass analyzer with reduced dwell times of 100 ms each.

#### *Methyl vinyl ketone and methacrolein branch emissions quantification with online thermal desorption GC-MS in parallel with real-time PTR-MS*

To quantitatively validate PTR-MS measurements of  $i_{\text{ox}}$ , quantification of methyl vinyl ketone and methacrolein concentrations in a branch enclosure was performed using an online thermal desorption GC-MS in parallel with real-time PTR-MS measurements of  $i_{\text{ox}}$ . Enclosure  $\text{CO}_2$  and  $\text{H}_2\text{O}$  concentrations were also monitored using a LI-7000. Detached mango branches in 20 mm pyruvate (1 branch), 20 mm pyruvate-2- $^{13}\text{C}$  (1 branch), 40 mm pyruvate (1 branch), and 40 mm pyruvate-2- $^{13}\text{C}$  (1 branch) solutions were placed in a 5 L Teflon branch enclosure with ~400 ppmv of dry hydrocarbon free air entering at 3 slpm. Light was supplied with an LED grow light at 1000–1500  $\mu\text{mol m}^{-2} \text{s}^{-1}$  PAR.

Methyl vinyl ketone and methacrolein were quantified using a Series 2 air server connected to a Unity 2 thermal desorption system (Markes International, Inc., Wilmington, DE, USA) interfaced with a 5975C series gas chromatograph/electron impact mass spectrometer with a triple-axis detector (Agilent Technologies). Samples (1.5 L) were pre-concentrated on an internal sorbent tube (water management cold trap, Markes International) held at 30 °C (to avoid excess water collection) and dried by purging with dry carrier gas at 20 sccm for 20 min. During injection, the trap was heated to 300 °C for 3 min while backflushing with carrier gas at a flow of 6.5 sccm. To improve peak shape and further reduce the amount of water introduced into the GC-MS, 5 sccm of this flow was vented through the split while the remaining 1.5 sccm was directed to the column (Agilent DB624 60 m  $\times$  0.32 mm  $\times$  1.8  $\mu\text{m}$ ), temperature programmed with an initial hold of 3 min at 40 °C followed by an increase to 230 °C at 6 °C  $\text{min}^{-1}$ . The mass spectrometer was configured for trace analysis (SIM Mode and 15 X detector gain factor) with 100 ms dwell times for the major methyl vinyl ketone ( $m/z$  43, 55, 70) and methacrolein ( $m/z$  39, 41, 70) fragment ions. In addition,  $m/z$  71 was included to calculate  $^{13}\text{C}/^{12}\text{C}$  ratios which are expected to be enhanced during the pyruvate-2- $^{13}\text{C}$  branch feeding. Calibration of the GC-MS to methyl vinyl ketone and methacrolein was accomplished using the dynamic solution injection technique with a methanol solution containing 2.4 mM of both methyl vinyl ketone and methacrolein. Identification of methyl vinyl ketone and methacrolein in enclosure air was confirmed by comparison of mass spectra with the standard and by comparison of retention times. An assessment of empty enclosure air (without a branch)

demonstrated that methyl vinyl ketone and methacrolein blanks were negligible.

### *Biosphere 2 tropical rainforest mesocosm*

The 2000 m<sup>2</sup> tropical rainforest mesocosm at Biosphere 2 currently encompasses 91 species of tropical plants from 41 families, including 73 trees under a flat-topped pyramidal glass enclosure operated as a semi-closed system. Branch enclosure air temperature and ambient air temperature along a vertical profile tower were continuously recorded. Eight 7–10 day measurement periods were made during January 22–April 14, 2010. The following species were analyzed for isoprene and  $i_{ox}$  emissions using branch enclosures in parallel with ambient air concentration measurements; *Mangifera indica*, *Pterocarpus indicus*, *Alpinia zerumbet*, *Hibiscus rosa-sinensis*, *Inga vera*, *Cissus sicyoides*, *Canna indica*, *Spathodea campanulata*, and *Phytolacca dioica*. Ambient air at mid height (13 m), zero air, zero air prior to entering a single 5 L branch enclosure flowing at 5.0 slpm, and branch enclosure air were analyzed (15 min each) continuously for isoprene and  $i_{ox}$  concentrations by PTR-MS. Air samples from the rainforest mesocosm were pumped through heated (50 °C) Teflon (PFA) tubing into the adjacent laboratory for trace gas analysis.

For single leaf gas exchange measurements of <sup>12</sup>C and <sup>13</sup>C isoprene and  $i_{ox}$  as well as CO<sub>2</sub> and H<sub>2</sub>O, a custom-built glass enclosure (volume ≈ 400 mL) with constant light (750 μmol m<sup>-2</sup> s<sup>-1</sup>) and temperature (30 °C) control was used as described previously (Jardine *et al.*, 2010c). Single mango tree leaves (*M. indica*) inside the rainforest mesocosm were removed, and the petioles were immediately recut under distilled water (two leaves), 44.7 mM sodium pyruvate (four leaves), sodium pyruvate-1-<sup>13</sup>C (one leaf), and 44.7 mM sodium pyruvate-2-<sup>13</sup>C (four leaves). Continuous measurements of <sup>12</sup>C and <sup>13</sup>C isoprene and  $i_{ox}$  emission rates were acquired for at least 12 h. Plant physiological variables like net carbon assimilation, transpiration, and stomatal conductance were also quantified.

### *BrazilianAir 2010 field campaign*

The BrazilianAir 2010 study was carried out at the TT34 tower (2°35.37'S, 60°06.92'W) in the Reserva Biológica do Cueiras in central Amazonia, 60 km NNW of the city of Manaus, Brazil. The site is run by INPA (Instituto Nacional de Pesquisas da Amazonia) under the Large Scale Biosphere–Atmosphere Experiment in Amazonia (LBA) program (Martin *et al.*, 2010). The vegetation in this area is considered to be undisturbed, mature, *terra firme* rainforest, with a leaf area index of 5–6 and an average canopy height of 30 m. The dry season measurements described in this manuscript occurred between 2 September 2010 and 5 December 2010. The site description, techniques for isoprene and  $i_{ox}$  vertical concentration measurements, and estimated source/sink distributions are previously described (Karl *et al.*, 2009). The only modification made to these methods was the use of heated gas inlets (50 °C) and measurements for 10 min at each of the six heights instead of 5 min resulting in one complete profile every hour.

### *Chemical kinetics model*

We constructed a simple chemical kinetics model using the simulation program STELLA (<http://www.iseesystems.com>) that simulated isoprene, ROS, and methyl vinyl ketone + methacrolein ( $i_{ox}$ ) metabolism in leaves. The units are not specified, nor are the actual values representative of real values. The goal of the qualitative analysis was to understand the processes that can impact the  $i_{ox}/i$  emission ratios from leaves. The isoprene reservoir (represents internal isoprene concentration in plants) was determined by production (given a diurnal pattern), emissions ( $g[\text{isoprene}]$ , where  $g$  is stomatal conductance), and oxidation ( $k[\text{ROS}][\text{isoprene}]$ , where  $k$  is the rate constant). Isoprene oxidation products  $i_{ox}$  were also given an internal plant reservoir which were determined by production (set equal to isoprene oxidation), emissions ( $g[i_{ox}]$ ), and consumption ( $c[i_{ox}]$ , where  $c$  is the consumption rate constant). ROS was also given its own reservoir with production and two loss processes including reaction with isoprene ( $k[\text{ROS}][\text{isoprene}]$ ) and 'other' nonisoprene related loss processes like enzyme scavenging and reaction with other antioxidants ( $o[\text{ROS}]$ , where  $o$  is the rate constant). ROS production rates were given a diurnal pattern (case 1) and a constant production rate (case 2).

## Results

### *Leaf and branch pyruvate feeding experiments*

Because pyruvate is a known precursor of isoprene in plants (Lichtenthaler *et al.*, 1997), we used leaf feeding of pyruvate, pyruvate-1-<sup>13</sup>C, and pyruvate-2-<sup>13</sup>C under constant light and temperature conditions to assess the possibility that isoprene oxidation within leaves leads to the formation and emission of  $i_{ox}$ . When petioles of single detached Mango leaves (four replicates) obtained from the rainforest mesocosm inside of Biosphere 2 were placed in a solution of pyruvate-2-<sup>13</sup>C, the measured carbon isotope ratios (<sup>13</sup>C/<sup>12</sup>C) of the subsequent isoprene and  $i_{ox}$  emissions were both elevated (relative to controls fed with distilled water, unlabeled pyruvate, and pyruvate-1-<sup>13</sup>C; Fig. 2 vs. Fig. 3). In addition, strong linear correlations were observed between <sup>13</sup>C- $i_{ox}$  emissions and <sup>13</sup>C-isoprene emissions ( $R^2 = 0.86$ – $0.96$  for the four replicates), providing evidence of in-leaf oxidation of isoprene to  $i_{ox}$  (Fig. 4).

Similar pyruvate and pyruvate-2-<sup>13</sup>C feeding experiments were performed using detached branches with simultaneous quantification of isoprene and  $i_{ox}$  using PTR-MS and online GC-MS (see GC-MS  $i_{ox}$  peaks from detached Mango branch emissions in Fig. 5). During pyruvate branch feeding, quantification of isoprene and  $i_{ox}$  concentrations and  $i_{ox}/i$  ratios were comparable between the two techniques (PTR-MS and GC-MS), and similar patterns were observed in both (Fig. 6).

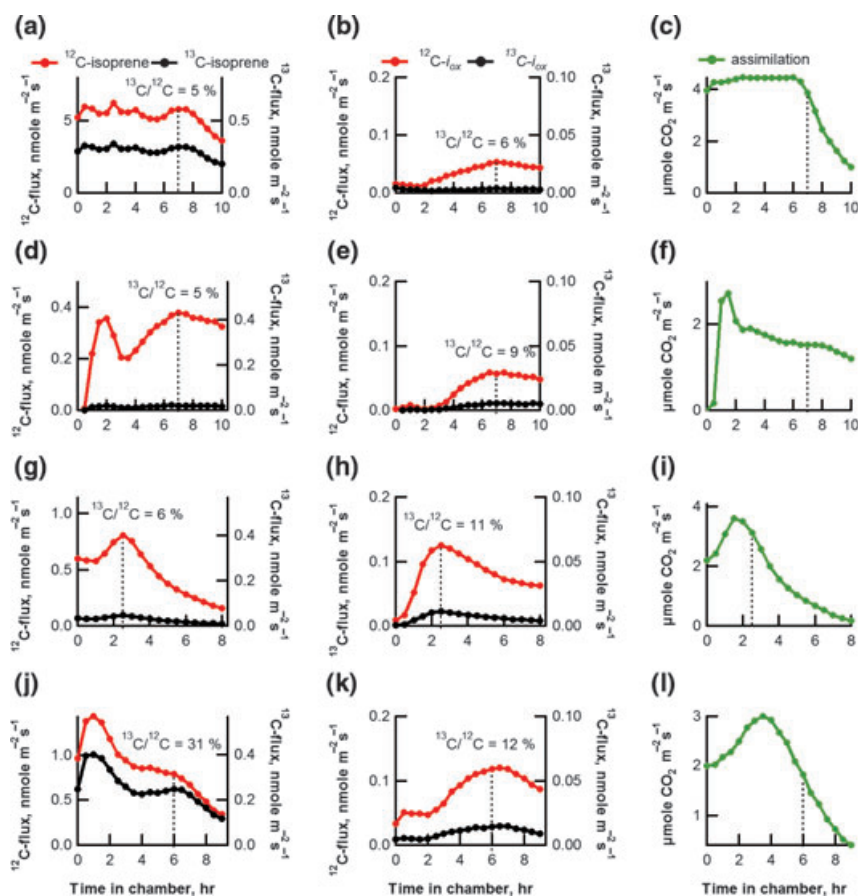


**Fig. 2** Control leaf feeding experiments with distilled water, unlabeled pyruvate, and pyruvate-1- $^{13}\text{C}$ .  $^{12}\text{C}$ -isoprene,  $^{13}\text{C}$ -isoprene,  $^{12}\text{C}$ - $i_{\text{ox}}$ , and  $^{13}\text{C}$ - $i_{\text{ox}}$  emission rates from mango leaves fed with distilled water (control: a–b; d–e), unlabeled pyruvate (control: g–h), and pyruvate-1- $^{13}\text{C}$  (control: j–k) through the transpiration stream. Net carbon assimilation is also shown for control and labeled leaves (c, f, i, l, o). The dashed line indicates timing of maximum  $^{12}\text{C}$ -isoprene flux, co-occurring with maximum  $^{12}\text{C}$ - $i_{\text{ox}}$  flux.

There is a similar general pattern for 20 and 40 mM pyruvate, with  $i_{\text{ox}}$  emissions initially decreasing followed by an increase and a decline. However, the final decline was not observed in the 20 mM solution likely because only 8 h of data were collected compared with 16 h for the 40 mM pyruvate solution. In addition,  $^{13}\text{C}/^{12}\text{C}$ -methacrolein ratios were determined from GC-MS mass spectra of the methacrolein peaks using the ratio of  $m/z$  71 to  $m/z$  70 signals ( $m/z$  71 corresponds to  $i_{\text{ox}}$  with one  $^{13}\text{C}$  atom in place of any of the four  $^{12}\text{C}$  atoms). Control branches fed with pyruvate emitted methacrolein with  $^{13}\text{C}/^{12}\text{C}$  within the range of the expected natural abundance value of  $^{13}\text{C}/^{12}\text{C}$  (4.4%) (isotope distribution calculator, <http://www.sisweb.com/mstools/isotope.htm>) (Fig. 7). In contrast, during pyruvate-2- $^{13}\text{C}$  branch feeding experiments, significant enrichments in  $^{13}\text{C}$ -methacrolein was observed with  $^{13}\text{C}/^{12}\text{C}$  ratios up to 30% (Fig. 7). Although  $i_{\text{ox}}$  emissions from mango were dominated by methacrolein, similar  $^{13}\text{C}$  enrichment in methyl vinyl ketone was also observed.

#### *Isoprene and $i_{\text{ox}}$ emissions from intact branches*

We then investigated whether we could detect isoprene and  $i_{\text{ox}}$  emissions from intact plants using individual branch enclosures. We found that seven of nine species of tropical plants investigated in the Biosphere 2 rain-forest mesocosm were net emitters of both isoprene ( $i$ ) and  $i_{\text{ox}}$ , and that  $i_{\text{ox}}$  and isoprene emissions increased with enclosure air temperature (see Supporting Information, Fig. S1). In addition,  $i_{\text{ox}}$  and isoprene emissions correlated well within branch measurements ( $R^2$ : range 0.50–0.97, mean 0.81), giving well-defined  $i_{\text{ox}}/i$  emissions ratios for each species (see examples in Fig. 8) which increased with maximum enclosure air temperature across species (Fig. 9a).

#### *Whole mesocosm ambient concentrations of isoprene and $i_{\text{ox}}$*

Simultaneously with the Biosphere 2 branch enclosure studies, we also analyzed ambient air from the enclosed

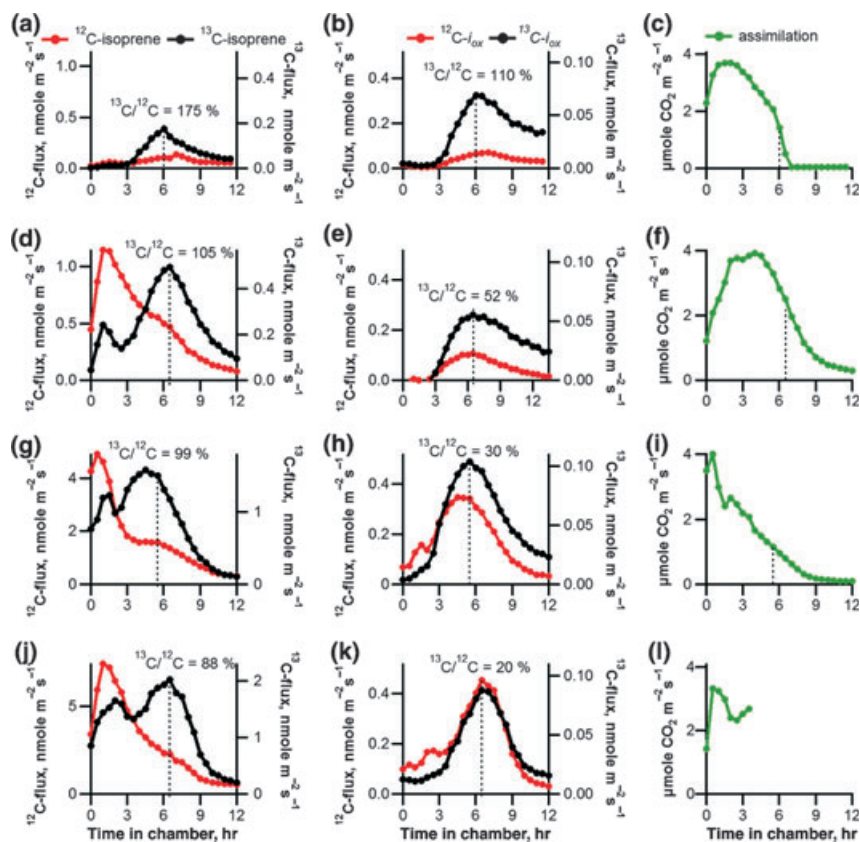


**Fig. 3** Pyruvate- $^{2-13}\text{C}$  leaf feeding experiments.  $^{12}\text{C}$ -isoprene,  $^{13}\text{C}$ -isoprene,  $^{12}\text{C}$ - $i_{\text{ox}}$  and  $^{13}\text{C}$ - $i_{\text{ox}}$  emission rates from mango leaves fed with pyruvate- $^{2-13}\text{C}$  through the transpiration stream. The labeling experiment was performed on four replicates (a–b; d–e; g–h; j–k). Net carbon assimilation is also shown (c, f, i, l, o). Carbon assimilation data stopped recording during the fourth replicate due to a software problem. The dashed line indicates timing of maximum  $^{13}\text{C}$ -isoprene flux, co-occurring with maximum  $^{13}\text{C}$  in  $i_{\text{ox}}$ .

rainforest mesocosm to determine if the same pattern could be observed at the scale of the whole 0.5 ha mesocosm. We took advantage of the fact that the glass structure at Biosphere 2 absorbs the ultraviolet photon flux needed for the generation of atmospheric oxidants (Pegoraro *et al.*, 2006). This enabled us to eliminate the complicating effects of gas-phase photooxidation of isoprene in the atmosphere and isolate the role of oxidation in plants, as under these conditions changes in ambient concentrations directly reflect changes in leaf-atmosphere fluxes. Ambient concentrations of  $i_{\text{ox}}$  showed strong diurnal patterns, which correlated with those of isoprene ( $R^2$ : range 0.66–0.99, mean 0.92) (Fig. 10a). GC-PTR-MS chromatograms of ambient air in the mesocosm demonstrate that the signal at  $m/z$  69 corresponds to a single peak (isoprene), whereas both methacrolein and methyl vinyl ketone contribute to the signal at  $m/z$  71 (Fig. 10b). Over the course of the 3 month study on whole mesocosm ambient air from winter to late spring, the  $i_{\text{ox}}/i$  concentration ratio increased with maximum ambient air temperatures ( $32\text{ }^\circ\text{C} \rightarrow 51\text{ }^\circ\text{C}$  at 20 m height) (Fig. 9b).

#### BrazilianAir 2010 field campaign

To determine if isoprene oxidation in plants could be detected in a natural primary rainforest with competing atmospheric isoprene oxidation, mean daytime ambient concentrations of isoprene and its oxidation products  $i_{\text{ox}}$  were quantified in central Amazonia during the 2010 dry season. While concentrations of isoprene peaked within the canopy, those of  $i_{\text{ox}}$  tended to be the highest at the top and above the canopy (Fig. 11a vs. 11b). As also observed in other forest ecosystems (Karl *et al.*, 2004), such a concentration profile suggests net ecosystem emissions of isoprene and uptake of  $i_{\text{ox}}$  (Fig. 11c vs. 11d). However, while isoprene emission rates inferred from concentrations were estimated to be highest near the top of the main canopy ( $\sim 28\text{ m}$ ) with a second, lower peak at the top of the sun-lit subcanopy ( $\sim 16\text{ m}$ ), the concentration profiles suggested two distinct regions of net  $i_{\text{ox}}$  uptake within the canopy just below the two peaks in isoprene emissions.

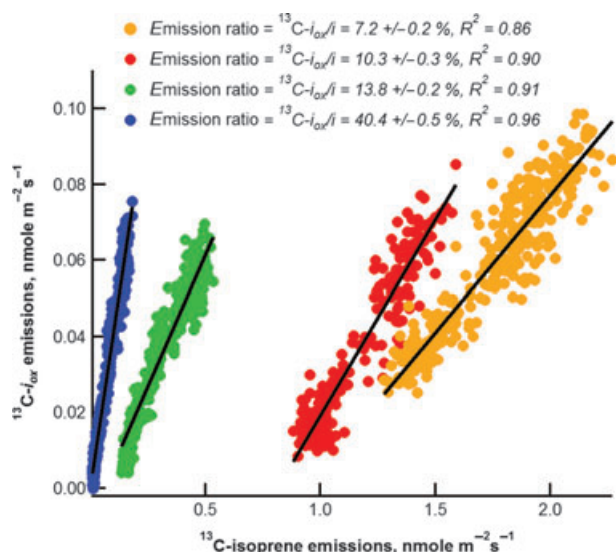


**Fig. 4** Linear correlations between  $^{13}\text{C}$ - $i_{\text{ox}}$  and  $^{13}\text{C}$ -isoprene emissions during the four replicate pyruvate- $^{13}\text{C}$  leaf feeding experiments shown in Fig. 3. Only data from the rise to the peak in  $i_{\text{ox}}$  emissions were included, when there was a strong linear relationship observed between  $^{13}\text{C}$ - $i_{\text{ox}}$  and  $^{13}\text{C}$ -isoprene emissions.

## Discussion

To interpret observed isoprene and  $i_{\text{ox}}$  dynamics from intact branches and whole ecosystems, we used a simple chemical kinetics model to simulate leaf isoprene, ROS, and  $i_{\text{ox}}$  metabolism. Our modeling results suggest that in a system where  $i_{\text{ox}}$  is exclusively produced from the oxidation of isoprene, changes in emission ratios ( $i_{\text{ox}}/i$ ) are solely driven by changes in ROS concentrations. ROS are known to accumulate in plants under virtually all stresses that impair primary metabolism

and linear electron transport (Suzuki & Mittler, 2006). Our modeling results suggest that under high ROS production rates, a higher fraction of isoprene is oxidized internally rather than emitted as whole isoprene molecules. This oxidized isoprene is further metabolized within plants or directly emitted as oxidation products  $i_{\text{ox}}$ . However, with ROS production rates held constant increased isoprene production rates result in a suppression of ROS concentrations due to increased loss from isoprene-ROS reactions. These modeling results support our experimental observations that  $i_{\text{ox}}/i$  emission ratios increase with maximum temperature (observed at the branch and whole mesocosm scales, temperature and light held constant at the leaf scale), but decrease with isoprene emission rates (observed at the leaf, branch, and whole mesocosm scales) and highlight the potential function of isoprene production in plants to suppress ROS. This apparent antioxidant role of isoprene at elevated temperatures might contribute to the mechanisms involved in the protective role of isoprene in thermotolerance (Sasaki *et al.*, 2007; Sharkey *et al.*, 2008). However, because we did not simultaneously quantify ROS concentrations in leaves, these conclusions remain speculative. Nevertheless, given that a substantial fraction of isoprene can be oxidized within leaves, the gross production of isoprene by plants must be larger than measured so far by enclosure and flux methods, especially when high emission and oxidation rates are simultaneously enhanced (e.g. by high temperatures).

Why would plants invest limited carbon substrates (that could be used to support growth and metabolism) so heavily in isoprene emissions only to recapture a fraction of its secondary photo-oxidation products from the atmosphere? The emerging picture from our experiments is that these processes occur because isoprene

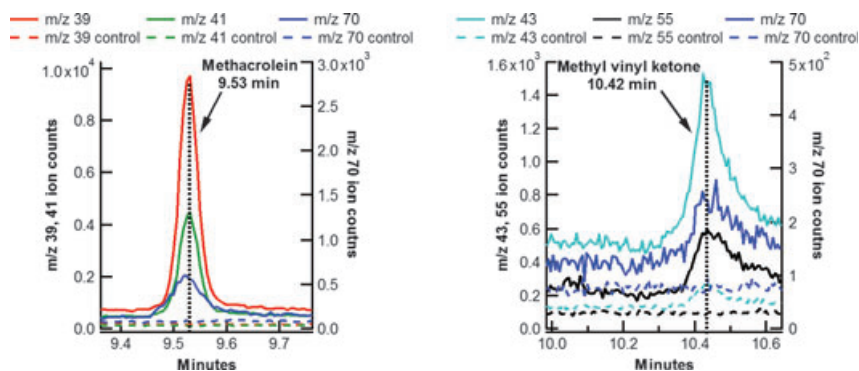


**Fig. 5** GC-MS chromatograms of air samples collected from an empty branch enclosure (control) and a detached mango branch placed in the branch enclosure with the stem in a 20 mM pyruvate solution. Signal peaks corresponding to the dominant ion fragments of methacrolein ( $m/z$  39, 41, 70) and methyl vinyl ketone ( $m/z$  43, 55, 70) were observed from the mango branch sample at the retention time of authentic standards.

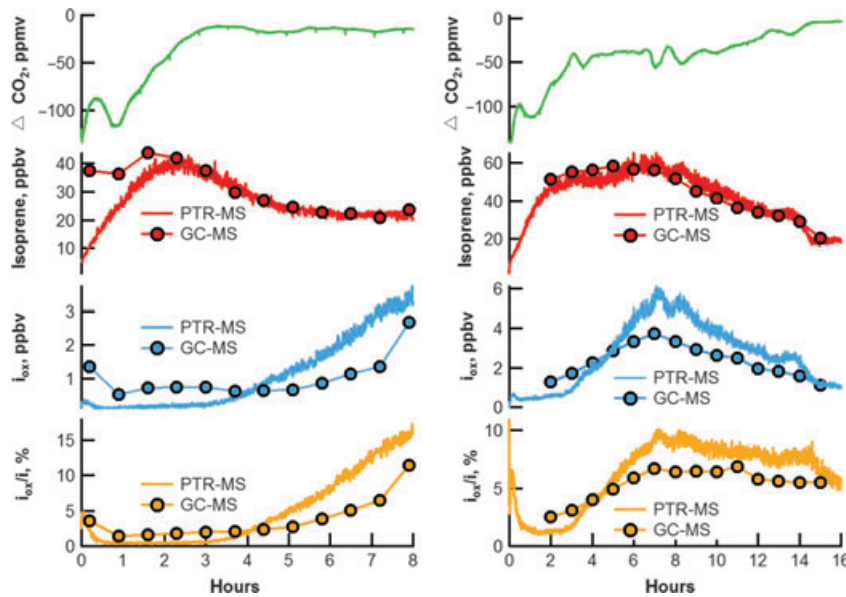


Fig. 6 Simultaneous GC-MS and PTR-MS emission measurements of isoprene,  $i_{ox}$ , and  $i_{ox}/i$  from mango branches in (a) 20 mM pyruvate and (b) 40 mM pyruvate solutions.  $CO_2$  uptake during photosynthesis is also shown.

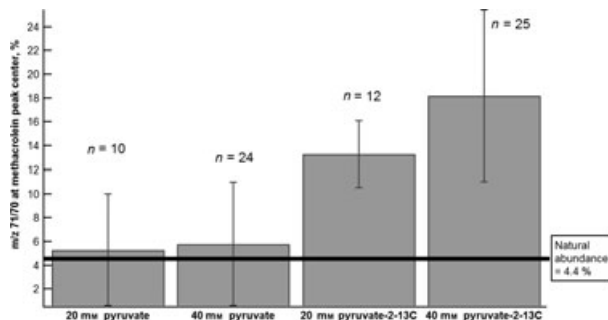


Fig. 7 Average  $^{13}C/^{12}C$  ratios of methacrolein determined by GC-MS from the ratio of the  $m/z$  71 to  $m/z$  70 signals of the methacrolein peaks obtained during pyruvate and pyruvate- $2-^{13}C$  feeding of detached mango branches. For each branch,  $N$  samples were analyzed with error bars representing 1 SD. Note the enrichment in  $^{13}C$  of methacrolein emitted from pyruvate- $2-^{13}C$  feeding relative to pyruvate feeding. Similar results were obtained for methyl vinyl ketone.

acts as an antioxidant in plants by directly reacting with ROS to produce  $i_{ox}$ , which are further metabolized, or emitted. As methyl vinyl ketone is cytotoxic (Vollenweider *et al.*, 2000), we believe that emission of  $i_{ox}$  plays a prominent role in detoxification. Conversion of isoprene to  $i_{ox}$  may allow for continued plant function through periods of abiotic and biotic stress that could otherwise reduce plant performance. Protection against ROS in plants is known to take place through several, often independent, enzymatic and nonenzymatic mechanisms that allow ROS scavenging (Ahmad *et al.*, 2008). However, many of these mechanisms are not in-phase

with daily peaks of ozone and ROS production (Fares *et al.*, 2010). Isoprene on the other hand also peaks during the central hours of the day due to a strong dependence of production rates on light and temperature (Guenther *et al.*, 2006), and isoprene-ROS reactions may therefore protect the metabolic structures within plant leaves by converting isoprene to  $i_{ox}$ . In the presence of atmospheric oxidants, isoprene oxidation in plants can be masked by net ecosystem uptake of  $i_{ox}$  driven by high ambient  $i_{ox}$  concentrations and effective sinks for  $i_{ox}$  in plants such as enzymatic oxidation via aldehyde dehydrogenase (Karl *et al.*, 2010). These processes along with the fact that  $i_{ox}$  emission rates are generally low, and the majority of past observations of  $i_{ox}$  production have been conducted in field studies, likely explains why plants are not generally considered significant atmospheric sources of  $i_{ox}$ . Consistent with our findings from tropical plants, primary emissions of  $i_{ox}$  have also been observed from Birch (Folkers *et al.*, 2002) and creosotebush (Jardine *et al.*, 2010a) leaves with strong light and temperature dependences.

In the Amazon, current dry deposition schemes would predict maximum  $i_{ox}$  dry deposition fluxes to occur at the top of the canopy and not within the canopy as observed (Fig. 11d). Because plants both produce and consume  $i_{ox}$ , they possess a compensation point that can be defined as the ambient atmospheric concentration of  $i_{ox}$  where the net exchange flux between plants and the atmosphere is zero. Ambient atmospheric concentrations above the compensation point result in net diffusion into the leaves, while those

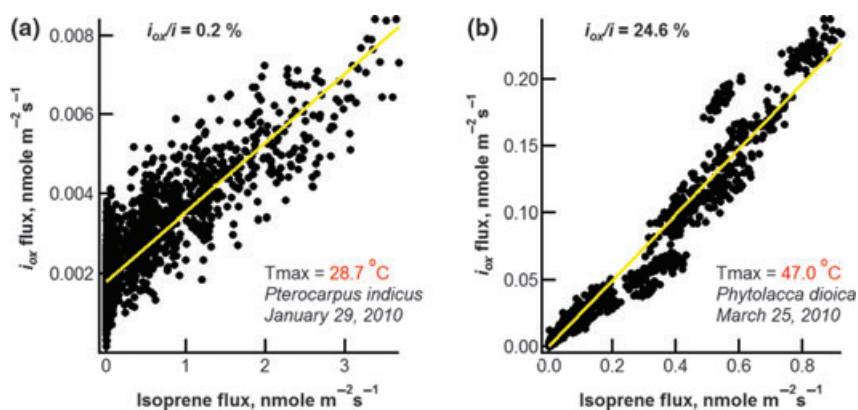


Fig. 8 Example scatter plots of  $i_{ox}$  vs. isoprene emission rates from 6 days of emission data from two tropical plants inside the rainforest mesocosm at Biosphere 2 exposed to different maximum enclosure air temperatures.

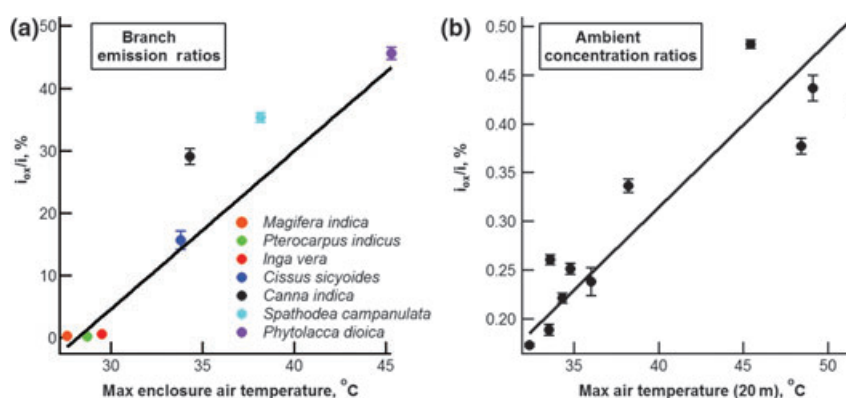
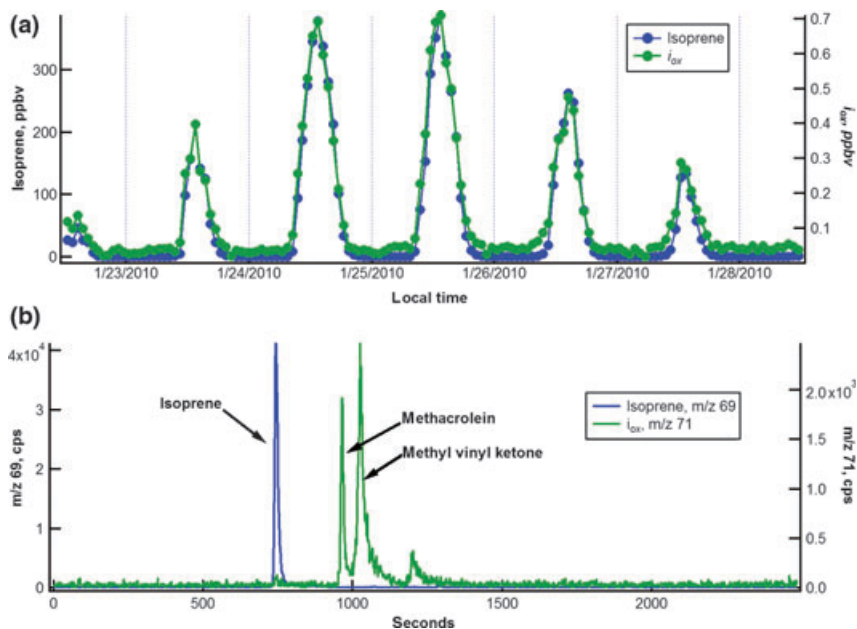


Fig. 9 Dependence of  $i_{ox}/i$  ratios ( $\pm 1$  SD) on maximum air temperature during the 7–10 day measurement period for individual branches and whole mesocosm ambient air (a) Branch  $i_{ox}/i$  emission ratios for seven different tropical plant species inside Biosphere 2 vs. maximum enclosure air temperature. (b) Whole mesocosm scale ambient  $i_{ox}/i$  concentration ratios inside the Biosphere 2 tropical rainforest mesocosm from winter to spring of 2010 vs. maximum air temperature at 20 m.

below the compensation point result in net emission flux (Kesselmeier, 2001). It has been shown that the compensation point of  $i_{ox}$  increases with temperature for *Populus deltoides*, which may be due to increased production rates relative to consumption rates within plants (Karl *et al.*, 2010). Generalizing these results to the Amazonian rainforest, we would explain the observed pattern of within canopy uptake of  $i_{ox}$  as follows; at the top of the canopy ( $\sim 30$  m) where temperature, light, and isoprene emissions are at a maximum,  $i_{ox}$  compensation points are elevated due to also high internal plant production from isoprene oxidation. Atmospheric oxidation of isoprene elevates ambient  $i_{ox}$  concentrations to near the compensation point, effectively suppressing net  $i_{ox}$  emissions at the top of the canopy. Slightly deeper in the canopy (22 m) in the shaded region of the upper canopy where isoprene emissions are much lower due to lower temperatures and light intensities,  $i_{ox}$  compensation points are lower

due to even more reduced internal production from isoprene oxidation, resulting in strong net uptake of  $i_{ox}$ .

In the central Amazon during the 2010 dry season, isoprene oxidation in the atmosphere dominated isoprene oxidation within plants and net ecosystem  $i_{ox}$  uptake was observed under the field conditions studied. However, within-plant isoprene oxidation in the sun-lit top of the canopy (30 m) shifted  $i_{ox}$  uptake fluxes to deeper within the canopy (Fig. 11). This is in contrast with individual plants in the Biosphere 2 tropical rainforest mesocosm where net  $i_{ox}$  emissions occurred due to the promotion of isoprene oxidation under elevated light and temperature stress and the use of zero air in the branch enclosures. This suggests that under conditions that favor elevated isoprene oxidation rates in plants (high abiotic stress) and reduced isoprene oxidation rates in the atmosphere (reduced oxidative capacity of the atmosphere), the biosphere could theoretically become a net source of  $i_{ox}$  to the



**Fig. 10** Ambient isoprene and  $i_{ox}$  inside the Biosphere 2 tropical rainforest mesocosm. (a) Diurnal patterns of isoprene and  $i_{ox}$  ambient concentrations quantified with PTR-MS during a 6 day period (b) GC-PTR-MS chromatogram of mesocosm ambient air during mid-day showing the presence of isoprene (m/z 69) and methyl vinyl ketone and methacrolein ( $i_{ox}$ , m/z 71).

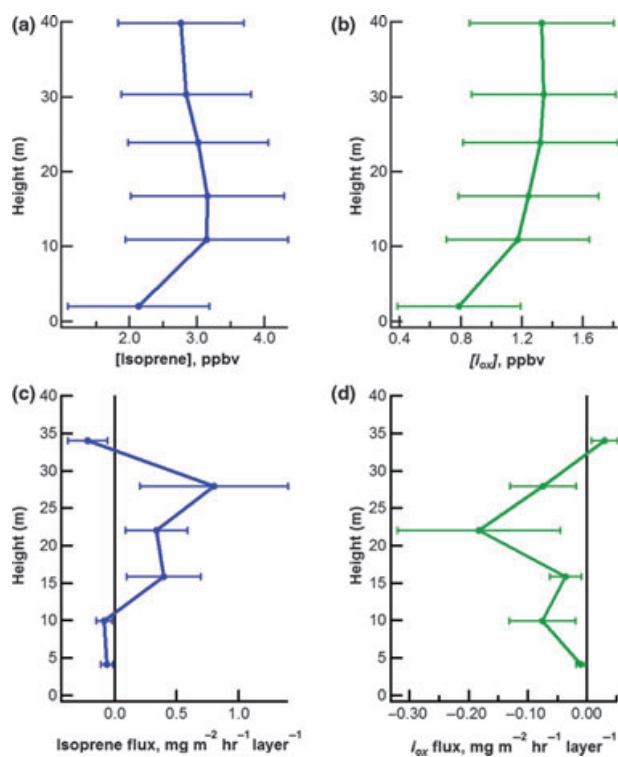


**Fig. 11** Concentrations (a, b) and estimated source/sink distributions (c, d)  $\pm 1$  SD of isoprene and  $i_{ox}$  through a 30 m canopy in central Amazonia during the 2010 dry season. Net emission fluxes are represented by positive values, whereas uptake fluxes are represented as negative values.

atmosphere. This has recently been reported from a tropical forest in Malaysia where  $i_{\text{ox}}$  production in the biosphere dominated production in the atmosphere resulting in small net ecosystem scale  $i_{\text{ox}}$  emissions instead of uptake (Langford *et al.*, 2010) with the highest ambient  $i_{\text{ox}}$  concentrations at the top of the canopy rather than above it (J. Ryder, unpublished data). These observations suggest a fundamental change in how we might need to treat isoprene and its oxidation products in future land-atmosphere exchange models to include its effects on both within plant and atmosphere  $i_{\text{ox}}$  production and their relative importance in driving the net direction and magnitude of ecosystem  $i_{\text{ox}}$  fluxes.

Photochemical models of isoprene oxidation used in current chemical transport models are based on reaction pathways determined from first-generation product data (i.e.  $i_{\text{ox}}$ ) acquired in laboratory experiments (Atkinson *et al.*, 1989). However, recent observations of OH and HO<sub>2</sub> concentrations in the remote troposphere (low NO<sub>x</sub>) are considerably higher than expected from chemical transport models, particularly in remote isoprene rich regions such as the Amazon Basin (Lelieveld *et al.*, 2008). This has prompted changes to the isoprene oxidation mechanisms used in chemistry-transport models to include various mechanisms of OH recycling (Stavrakou *et al.*, 2010). However, if a significant fraction of atmospheric  $i_{\text{ox}}$  is derived from isoprene oxidation within plants rather than isoprene oxidation in the atmosphere, the OH consumption will be overestimated resulting in higher than expected OH concentrations. To more thoroughly evaluate the importance of biogenic and atmospheric  $i_{\text{ox}}$  sources and sinks, new vertically resolved isoprene and  $i_{\text{ox}}$  concentration and flux observations are needed throughout a variety of natural and managed landscapes under a wide range of environmental conditions ranging from optimal conditions for plant growth and reproduction to abiotic stress under environmental extremes.

## Acknowledgements

Funding for this project was provided by the Philecology Foundation of Fort Worth, Texas, and the National Science Foundation through the AMAZON-PIRE (Partnerships for International Research and Education) award (0730305) and instrumentation support (CHE 0216226). The funders had no role in study design, data collection and analysis, decision to publish, or preparation of the manuscript. We would like to thank many individuals at the Instituto Nacional de Pesquisas da Amazônia (INPA) in Manaus, Brazil, for logistics support including Eliane Gomes Alves, Erika Schloemp, and Antonio Manzi.

## References

Ahmad P, Sarwat M, Sharma S (2008) Reactive oxygen species, antioxidants and signaling in plants. *Journal of Plant Biology*, **51**, 167–173.

- Apel K, Hirt H (2004) Reactive oxygen species: metabolism, oxidative stress, and signal transduction. *Annual Review of Plant Biology*, **55**, 373–399.
- Atkinson R, Baulch DL, Cox RA, Hampson RF, Kerr JA, Troe J (1989) Evaluated kinetic and photochemical data for atmospheric chemistry: supplement II. *Journal of Physical and Chemical Reference Data*, **18**, 881–1097.
- Dreyfus GB, Schade GW, Goldstein AH (2002) Observational constraints on the contribution to isoprene oxidation to ozone production on the western slope of the Sierra Nevada, California. *Journal of Geophysical Research-Atmospheres*, **107**, 4365–4381.
- Fares S, Goldstein A, Loreto F (2010) Determinants of ozone fluxes and metrics for ozone risk assessment in plants. *Journal of Experimental Botany*, **61**, 629–633.
- Folkers A, Koppmann R, Wildt J (2002) Direct emission of methyl vinyl ketone from Birch. In American Geophysical Union, Fall Meeting 2002, Vol. abstract A61B-0070. San Francisco.
- Guenther A, Karl T, Harley P, Wiedinmyer C, Palmer PI, Geron C (2006) Estimates of global terrestrial isoprene emissions using MEGAN (Model of Emissions of Gases and Aerosols from Nature). *Atmospheric Chemistry and Physics*, **6**, 3181–3210.
- Jardine K, Abrell L, Kurc SA, Huxman T, Ortega J, Guenther A (2010a) Volatile organic compound emissions from *Laurea tridentata* (creosotebush). *Atmospheric Chemistry and Physics*, **10**, 12191–12206.
- Jardine K, Henderson W, Huxman T, Abrell L (2010b) Dynamic solution injection: a new method for preparing pptv & ppbv standard atmospheres of volatile organic compounds. *Atmospheric Measurement Techniques*, **3**, 1569–1576.
- Jardine K, Sommer E, Saleska S, Huxman T, Harley P, Abrell L (2010c) Gas phase measurements of pyruvic acid and its volatile metabolites. *Environmental Science and Technology*, **44**, 2454–2460.
- Karl T, Potosnak M, Guenther A, Clark D, Walker J, Herrick JD, Geron C (2004) Exchange processes of volatile organic compounds above a tropical rain forest: implications for modeling tropospheric chemistry above dense vegetation. *Journal of Geophysical Research-Atmospheres*, **109**, D18306.
- Karl T, Guenther A, Turnipseed A, Tyndall G, Artaxo P, Martin S (2009) Rapid formation of isoprene photo-oxidation products observed in Amazonia. *Atmospheric Chemistry and Physics*, **9**, 7753–7767.
- Karl T, Harley P, Emmons L *et al.* (2010) Efficient atmospheric cleansing of oxidized organic trace gases by vegetation. *Science*, **330**, 816–819.
- Kesselmeier J (2001) Exchange of short-chain oxygenated volatile organic compounds (VOCs) between plants and the atmosphere: a compilation of field and laboratory studies. *Journal of Atmospheric Chemistry*, **39**, 219–233.
- Langford B, Misztal PK, Nemitz E *et al.* (2010) Fluxes and concentrations of volatile organic compounds from a South-East Asian tropical rainforest. *Atmospheric Chemistry and Physics*, **10**, 8391–8412.
- Lelieveld J, Butler TM, Crowley JN *et al.* (2008) Atmospheric oxidation capacity sustained by a tropical forest. *Nature*, **452**, 737–740.
- Lichtenthaler HK, Rohmer M, Schwender J (1997) Two independent biochemical pathways for isopentenyl diphosphate and isoprenoid biosynthesis in higher plants. *Physiologia Plantarum*, **101**, 643–652.
- Loreto F, Schnitzler JP (2010) Abiotic stresses and induced BVOCs. *Trends in Plant Science*, **15**, 154–166.
- Loreto F, Velikova V (2001) Isoprene produced by leaves protects the photosynthetic apparatus against ozone damage, quenches ozone products, and reduces lipid peroxidation of cellular membranes. *Plant Physiology*, **127**, 1781–1787.
- Loreto F, Mannozi M, Maris C, Nascetti P, Ferranti F, Pasqualini S (2001) Ozone quenching properties of isoprene and its antioxidant role in leaves. *Plant Physiology*, **126**, 993–1000.
- Martin ST, Andreae MO, Althausen D *et al.* (2010) An overview of the Amazonian Aerosol Characterization Experiment 2008 (AMAZE-08). *Atmospheric Chemistry and Physics*, **10**, 11415–11438.
- Moller IM (2001) Plant mitochondria and oxidative stress: electron transport, NADPH turnover, and metabolism of reactive oxygen species. *Annual Review of Plant Physiology and Plant Molecular Biology*, **52**, 561–591.
- Monson RK (2002) Volatile organic compound emissions from terrestrial ecosystems: a primary biological control over atmospheric chemistry. *The Israel Journal of Chemistry*, **42**, 29–42.
- Montzka SA, Trainer M, Goldan PD, Kuster WC, Fehsenfeld FC (1993) Isoprene and its oxidation-products, methyl vinyl ketone and methacrolein, in the rural troposphere. *Journal of Geophysical Research-Atmospheres*, **98**, 1101–1111.
- Pegoraro E, Rey A, Abrell L, Vanharen J, Lin GH (2006) Drought effect on isoprene production and consumption in Biosphere 2 tropical rainforest. *Global Change Biology*, **12**, 456–469.
- Pierotti D, Wofsy SC, Jacob D, Rasmussen RA (1990) Isoprene and its oxidation-products - methacrolein and methyl vinyl ketone. *Journal of Geophysical Research-Atmospheres*, **95**, 1871–1881.

- Sasaki K, Saito T, Lamsa M *et al.* (2007) Plants utilize isoprene emission as a thermo-tolerance mechanism. *Plant and Cell Physiology*, **48**, 1254–1262.
- Sharkey TD, Wiberley AE, Donohue AR (2008) Isoprene emission from plants: why and how. *Annals of Botany-London*, **101**, 5–18.
- Stavrakou T, Peeters J, Muller JF (2010) Improved global modelling of HO(x) recycling in isoprene oxidation: evaluation against the GABRIEL and INTEX-A aircraft campaign measurements. *Atmospheric Chemistry and Physics*, **10**, 9863–9878.
- Suzuki N, Mittler R (2006) Reactive oxygen species and temperature stresses: a delicate balance between signaling and destruction. *Physiologia Plantarum*, **126**, 45–51.
- Tani A, Tobe S, Shimizu S (2010) Uptake of methacrolein and methyl vinyl ketone by tree saplings and implications for forest atmosphere. *Environmental Science & Technology*, **44**, 7096–7101.
- Velikova V, Edreva A, Loreto F (2004) Endogenous isoprene protects *Phragmites australis* leaves against singlet oxygen. *Physiologia Plantarum*, **122**, 219–225.
- Velikova V, Pinelli P, Pasqualini S, Reale L, Ferranti F, Loreto F (2005) Isoprene decreases the concentration of nitric oxide in leaves exposed to elevated ozone. *New Phytologist*, **166**, 419–426.
- Vickers CE, Gershenzon J, Lerdau MT, Loreto F (2009) A unified mechanism of action for volatile isoprenoids in plant abiotic stress. *Nature Chemical Biology*, **5**, 283–291.
- Vollenweider S, Weber H, Stolz S, Chetelat A, Farmer EE (2000) Fatty acid ketodienes and fatty acid ketotrienes: Michael addition acceptors that accumulate in wounded and diseased *Arabidopsis* leaves. *Plant Journal*, **24**, 467–476.
- Warneke C, Holzinger R, Hansel A *et al.* (2001) Isoprene and its oxidation products methyl vinyl ketone, methacrolein, and isoprene related peroxides measured online over the tropical rain forest of Surinam in March 1998. *Journal of Atmospheric Chemistry*, **38**, 167–185.
- Warneke C, De Gouw JA, Kuster WC, Goldan PD, Fall R (2003) Validation of atmospheric VOC measurements by proton-transfer-reaction mass spectrometry using a gas-chromatographic pre-separation method. *Environmental Science and Technology*, **37**, 2494–2501.
- Young PJ, Arneth A, Schurgers G, Zeng G, Pyle JA (2009) The CO<sub>2</sub> inhibition of terrestrial isoprene emission significantly affects future ozone projections. *Atmospheric Chemistry and Physics*, **9**, 2793–2803.

### Supporting Information

Additional Supporting Information may be found in the online version of this article:

**Figure S1.** Branch  $i_{\text{ox}}$  (left  $y$ -axis) and isoprene (right  $y$ -axis) emissions vs. enclosure air temperature for various species inside the rainforest mesocosm at Biosphere 2. The bottom right panel is data collected in the Sonoran desert from creosotebush (*Larrea tridentata*) (Jardine *et al.*, 2010a). Data are fit to the function  $i_{\text{ox}}$  emissions =  $A_0 T^{\text{power}}$ .

Please note: Wiley-Blackwell are not responsible for the content or functionality of any supporting materials supplied by the authors. Any queries (other than missing material) should be directed to the corresponding author for the article.